Title: An *in vitro* assay to investigate venom neurotoxin activity on muscle-type nicotinic acetylcholine receptor activation and for the discovery of toxin-inhibitory molecules

Authors: Rohit N Patel[1,2], Rachel H Clare[1,2], Line Ledsgaard[3], Mieke Nys[4], Jeroen Kool[5], Andreas H Laustsen[3], Chris Ulens[4] & Nicholas R Casewell[1,2]*

*** Corresponding Author:** Nicholas R Casewell

Affiliations:

[1]Centre for Snakebite Research & Interventions, Liverpool School of Tropical Medicine, L3 5QA, UK

[2]Department of Tropical Disease Biology, Liverpool School of Tropical Medicine, L3 5QA, UK

[3]Department of Biotechnology and Biomedicine, Technical University of Denmark, Kongens Lyngby, Denmark

[4]Laboratory of Structural Neurobiology, Department of Cellular and Molecular Medicine, Faculty of Medicine, KU Leuven, Belgium

[5]AIMMS Division of BioAnalytical Chemistry, Vrije Universiteit Amsterdam, Netherlands.

Categories: Neuropharmacology and Toxicology

Abstract

Snakebite envenoming is a neglected tropical disease that causes over 100,000 deaths annually. Envenomings result in variable pathologies, but systemic neurotoxicity is among the most serious and is currently only treated with difficult to access and variably efficacious commercial antivenoms. Venom-induced neurotoxicity is often caused by α-neurotoxins antagonising the muscle-type nicotinic acetylcholine receptor (nAChR), a ligand-gated ion channel. Discovery of therapeutics targeting α-neurotoxins is hampered by relying on binding assays that do not reveal restoration of receptor activity or more costly and/or lower throughput electrophysiology-based approaches. Here, we report the validation of a screening assay for nAChR activation using immortalised TE671 cells expressing the γ-subunit containing muscle-type nAChR and a fluorescent dye that reports changes in cell membrane potential. Assay validation using traditional nAChR agonists and antagonists, which either activate or block ion fluxes, was consistent with previous studies. We then characterised antagonism of the nAChR by a variety of elapid snake venoms that cause muscle paralysis in snakebite victims, before defining the toxin-inhibiting activities of commercial antivenoms, and new types of snakebite therapeutic candidates, namely monoclonal antibodies, decoy receptors, and small molecules. Our findings show robust evidence of assay uniformity across 96-well plates and highlight the amenability of this approach for the future discovery of new snakebite therapeutics via screening campaigns. The described assay therefore represents a useful first-step approach for identifying α-neurotoxins and their inhibitors in the context of snakebite envenoming, and it should provide wider value for studying modulators of nAChR activity from other sources.

Keywords: snake venom neurotoxin, α-neurotoxins, antivenom, nicotinic acetylcholine receptor (nAChR), three-finger toxin, antibody discovery, drug discovery

1. Introduction

Snakebite envenoming is a neglected tropical disease that is responsible for causing over 100,000 deaths and 400,000 disabilities each year [1]. To achieve the targets set out in the World Health Organization's (WHO's) snakebite roadmap to halve deaths and disability by 2030, more effective, affordable, and accessible treatments are urgently needed [2]. However, snake venom variation acts as a barrier to the development of broadly effective therapeutics because inter-specific toxin variation results in a diversity of pathogenic drug targets that cause variable envenoming pathologies in snakebite victims, *i.e.*, haemotoxicity, cytotoxicity, and/or neurotoxicity [3]. Snake venom composition is dictated by variable representation by several toxin families, such as snake venom metalloproteinases (SVMPs), snake venom serine proteases (SVSPs), phospholipases A_2 (PLA_2s), and three-finger toxins (3FTxs) [4]. The latter two are usually of greatest significance in medically important elapid snake venoms [5], with highly abundant 3FTx isoforms often responsible for causing potentially lethal systemic neurotoxicity [6].

3FTxs are broadly subdivided by their structure and site of action into different subcategories. 3FTxs that exert their activity by binding to nicotinic acetylcholine receptors (nAChRs) located on the post-synaptic membranes of neuromuscular junctions are collectively known as α-neurotoxins (α-NTxs) [7]. α-NTxs are further subdivided based on their structure into long-chain (Lc-α-NTx), short-chain (Sc-α-NTx), non-conventional, and weak α-NTxs [6]. nAChRs are pentameric ligand-gated ion channels gated by the binding of the neurotransmitter acetylcholine (ACh) [8]. The nAChR located at the neuromuscular junction (referred to as 'muscle-type') consists of a combination of two α1 subunits with β1, δ, and either a γ subunit during foetal development (foetal) or a ε subunit thereafter (adult) [9]. Muscle-type nAChR activation results in skeletal muscle contraction, while binding of α-NTxs, which bind with high affinity and can have lengthy dissociation times [10], prevents activation by blocking ACh

71 binding, resulting in neurotoxicity, which presents clinically in snakebite victims as ptosis,
72 muscular paralysis, and respiratory depression [11,12].

73 Commercially available antivenoms are the only approved specific treatment for
74 snakebite envenoming. They consist of polyclonal antibodies purified from the plasma/sera of
75 animals immunised with sub-toxic doses of venom [13] and have proven to be effective at
76 preventing life-threatening signs of systemic envenoming if delivered promptly [14]. However,
77 current antivenoms have several limitations associated with them, including poor dose efficacy,
78 limited cross-snake species efficacy, high frequency of adverse reactions due to their
79 heterologous nature, and low affordability and accessibility to tropical snakebite victims
80 [15,16].

81 In recent years, several new approaches to either improve, supplement, or replace
82 existing antivenoms have been described [17–21]. Because neurotoxic envenoming can rapidly
83 become life-threatening, toxins that act on the nAChR are priority targets for the discovery of
84 novel therapeutics. Investigation of snake toxin action on nAChR functioning is traditionally
85 carried out using electrophysiological recordings [22] and/or recordings from *ex vivo* nerve-
86 muscle preparations [23]. However, these techniques are laborious, low-throughput, and
87 resource-intensive, and are therefore barriers to identifying novel neurotoxin-inhibiting
88 molecules (*e.g.*, monoclonal antibodies, peptides, and/or small molecule drugs). More recently,
89 automated patch-clamping has been introduced as a high-throughput method that allows for
90 similar types of electrophysiological recordings [24–26]. However, this approach requires
91 sophisticated equipment that is not available in most laboratories. Alternative methods to
92 investigate toxin-nAChR interactions have been developed, including the use of mimotopes of
93 the α1 nAChR subunit toxin binding site [27], a binding assay using purified nAChR from the
94 electric organ of *Torpedo* species [28], and the use of acetylcholine binding protein (AChBP),

a soluble protein from mollusc species, as a proxy for the nAChR [29]. However, each of these alternative approaches examines receptor binding rather than functionality.

A promising approach using immortalised TE671 cells expressing the foetal muscle-type nAChR [30] and a membrane potential dye to report receptor activation [31] has been used to investigate the activity of a Lc-α-NTx isolated from black mamba (*Dendroaspis polylepis*) venom [32]. The membrane potential dye moves intracellularly due to cation influx after receptor activation and binds to intracellular proteins and lipids resulting in an increase in fluorescence. This allows measurements of nAChR activation using an affordable plate reader and without the need for specialised electrophysiology equipment or facilities. TE671 cells have been widely used to investigate muscle-type nAChR function using patch-clamp electrophysiology [33–35] and, with membrane potential dye, have been used to investigate the nAChR activity of natural compounds [36–38], and to identify neuronal nAChR antagonists of relevance for tobacco addiction [39]. In this study, we exploited the assay potential of TE671 cells incubated with a membrane potential dye and validated this approach as a tool for: i) characterising the nAChR antagonism of crude snake venoms and isolated snake venom toxins, and ii) use as a 96-well plate *in vitro* assay platform for the discovery of novel toxin-inhibiting therapeutics (Fig. 1).

2. Experimental procedures

2.1 Materials

2.1.1 Venoms

Crude venoms were extracted from adult wild-caught specimens maintained in the herpetarium facility of the Centre for Snakebite Research & Interventions at the Liverpool School of Tropical Medicine (LSTM) (Liverpool, UK). The facility and its protocols for the

husbandry of snakes are approved and inspected by the UK Home Office and the LSTM and University of Liverpool Animal Welfare and Ethical Review Boards. Venoms of the following elapid snake species listed with their common name and country of origin were used: *Dendroaspis polylepis* (black mamba, Tanzania), *Dendroaspis viridis* (Western green mamba, Togo), *Dendroaspis angusticeps* (Eastern green mamba, Tanzania), *Dendroaspis jamesoni jamesoni* (Jameson's mamba, western subspecies, Cameroon), *Dendroaspis jamesoni kaimosae* (Jameson's mamba, eastern subspecies, Uganda), *Naja haje* (Egyptian cobra, Uganda), *Naja subfulva* (brown forest cobra, Uganda), and *Naja nivea* (cape cobra, South Africa). After extraction, venoms were immediately stored at -20 °C, lyophilised overnight, and stored long-term at 4 °C. Subsequent lyophilised extractions from each specimen were pooled with previous extractions. Concentrated stock solutions were created by reconstituting the lyophilised powder in PBS (10010023, Gibco, Thermo Fisher Scientific, Paisley, UK) and stored at -80 °C. Concentrations of venoms used in all experiments are expressed as the dry mass of lyophilised venom per mL of diluent.

2.1.2 nAChR agonists and antagonists

The following nAChR agonists were commercially acquired: acetylcholine chloride (A6625, Sigma-Aldrich, Gillingham, UK), nicotine ditartrate (GSK5294, Sigma-Aldrich, Gillingham, UK), and epibatidine dihydrochloride (AOB5901, Aobius, Gloucester, MA, USA). The Sc-α-NTx 'SHORT NEUROTOXIN alpha (NP)' (listed with the recommended name 'short neurotoxin 1' (sNTx1) on the UniProt database; P01426) isolated from *Naja pallida* venom was purchased from Latoxan (L8101, Valence, France), and the Lc-α-NTx, 'α-bungarotoxin' (α-BgTx), isolated from *Bungarus multicinctus* venom was purchased from Biotium (0010-1, Fremont, CA, USA).

2.1.3 Toxin-inhibiting molecules

The polyclonal antibody-based antivenoms EchiTAbG (batch EOG001740, expiry date October 2018, MicroPharm, Newcastle Emlyn, UK) and SAIMR (South African Institute for Medical Research) Polyvalent Snake antivenom (batch BF00546, expiry date November 2017, South African Vaccine Producers [SAVP], Johannesburg, South Africa) were obtained from the LSTM herpetarium via donation from Public Health England (London, UK). AChBP from *Lymnaea stagnalis* (*Ls*-AchBP) was prepared as previously described [17], as were the fully human monoclonal antibodies (mAbs) 2551_01_A12, 2554_01_D11 and 367_01_H01 in IgG1 format [21]. Samples of the various small molecule drugs used for screening were obtained by request from the Open Chemical Repository of the Developmental Therapeutics Program (https://dtp.cancer.gov) (Division of Cancer Treatment and Diagnosis, National Cancer Institute, Rockville, MD, USA), except for nicotine (see section 2.1.2) and varespladib (SML1100, Sigma-Aldrich, Gillingham, UK). These were selected based on their implied potential as α-NTx-inhibitors in previous studies [40–42]. Stock solutions of small molecules were created using dimethyl sulfoxide (DMSO) (D8418, Sigma-Aldrich, Gillingham, UK), and working solutions did not exceed 1% DMSO.

2.1.4 Cell line

The immortalised TE671 cell line (RRID: CVCL_1756) as used in Ngum et al. [43] was gifted by Dr Ian Mellor (University of Nottingham, UK) and originally obtained from the European Collection of Authenticated Cell Cultures (ECACC; catalogue no. 89071904). TE671 is a rhabdomyosarcoma cell line that natively expresses the foetal muscle-type nAChR (γ-subunit containing) [30].

2.2 Culture of TE671 cells

All further reagents were acquired from Gibco, Thermo Fisher Scientific, Paisley, UK, unless stated otherwise. TE671 cells were maintained using a culture medium consisting of

DMEM (high glucose, with GlutaMAX supplement, 10566016) supplemented with 10% FBS (qualified, Brazil origin, 10270106) and 1% penicillin-streptomycin solution (5000 units/mL penicillin, 5 mg/mL streptomycin, 15070063). Cells were cultured in 75 cm^2 cell culture flasks (83.3911, Sarstedt, Nümbrecht, Germany) and incubated at 37 °C/5% CO_2 until ~90% confluence was reached, upon which cells were dislodged from the flask with 4 mL TrypLE express enzyme (1x, no phenol red, 12604013). The suspension was added to 10 mL culture medium and centrifuged for 5 minutes (min) at 300 x g. The supernatant was removed, and the pellet resuspended in 5 mL culture medium. Cell suspensions of different flasks were pooled, counted using an automated cell counter (Luna II, Logos Biosystems, Villeneuve-d'Ascq, France) and further culture medium added to reach a count of $3x10^4$-$4x10^4$ cells/100 µL. Next, 100 µL cell suspension was pipetted to the wells of black walled, clear bottom, tissue culture treated 96-well plates (655090, Greiner Bio One, Stonehouse, UK) and incubated overnight at 37 °C/5% CO_2.

2.3 Membrane potential assay of nAChR activation

The following method was adapted from Fitch et al. [24] and Wang et al. [25] and, as in section 2.2, all reagents were acquired from Gibco, Thermo Fisher Scientific, Paisley, UK, unless stated otherwise. One vial of FLIPR membrane potential dye (Component A, Explorer Kit Blue, R8042, Molecular Devices, San Jose, CA, USA) was dissolved in 36 mL assay buffer to create the dye solution. Assay buffer consisted of 1x HBSS (made from 10x solution [14065049] as per manufacturer's instruction by diluting with distilled water and addition of $NaHCO_3$ [7.5% solution, 25080094] to a final concentration of 4.17 mM) supplemented with 20 mM HEPES (1 M solution, 15630056), 0.5 µM atropine (A0132, Sigma-Aldrich, Gillingham, UK), adjusted to pH 7.1 with 1 M NaOH, and then sterile filtered. Assay buffer was then used to create all further solutions. Culture medium was removed from the cell plate, replaced with 50 µL dye solution and incubated for 30 min at 37 °C/5% CO_2. When

192 investigating venom/toxin inhibition, the solutions of venom, toxin, toxin-inhibitor, or
193 combinations thereof were concurrently incubated for 30 min at 37 °C/5% CO_2 prior to addition
194 to the cell plate. Next, 50 µL of control or venom/toxin or venom/toxin + toxin-inhibitor
195 solutions were transferred to each well, and the cell plate further incubated for 15 min at 37
196 °C/5% CO_2. The cell plate was then acclimatised for 15 min at room temperature before
197 recording. Next, 60 µL nAChR agonist solution or assay buffer was added to the wells of a
198 clear, v-bottom 96-well plate (651201, Greiner Bio One, Stonehouse, UK) to create a reagent
199 plate and was then added to the appropriate tray, along with the cell plate and a rack of pipette
200 tips (black, 96-well configuration, 9000-0911, Molecular Devices, San Jose, CA, USA), to a
201 FlexStation 3 multi-mode microplate reader (Molecular Devices, San Jose, CA, USA)
202 controlled by SoftMax Pro 7.1 software (Molecular Devices, San Jose, CA, USA). The reader
203 records a column of the 96 well plate for a time set by the user and houses an automated
204 pipetting system that allows the addition of solution from the reagent plate to the cell plate at
205 a set time during the recording. After the column is recorded the adjacent column is then
206 recorded in the same manner. For the purposes of this study this allowed a baseline recording
207 followed by the addition of an agonist solution and the recording of changes in dye fluorescence
208 immediately following this addition. Excitation, cut-off, and emission wavelengths were set at
209 530, 550, and 565 nm respectively. Recordings of plates were carried out at room temperature
210 using a reading time of 214 seconds (s) and interval time of 2 s to give a total of 108 readings
211 per well with compound transfer (addition of agonist solution) of 50 µL to each well after 20 s
212 baseline recording.

213 **2.4 Data and Statistical Analysis**

214 Fluorescent responses for each well were measured by the software in relative
215 fluorescent units (RFUs), and values were determined by calculating the baseline fluorescence
216 ($F_{baseline}$, the mean of the first 20 s of responses) and subtracting this from the maximum

fluorescent response (F_{max}) for the remainder of the recording for each well (F_{max}- $F_{baseline}$). As different wells can have different starting RFU values, this normalisation approach ensured that the responses detected from each well could be compared on the same scale.

For experiments to profile agonists and antagonists, assay buffer alone was included as a control. For all subsequent work, 10 µM ACh was used as the control agonist, and all data points normalised to this agonist alone control. For experiments with isolated α-NTxs, 10 µM ACh was applied after incubation with varying concentrations of toxin. Crude venom experiments were carried out and normalised in the same way. Experiments with toxin-inhibitors included the ACh control (agonist alone), antagonist (venom or toxin) + ACh, and toxin-inhibitor + ACh. The screen of a panel of potential small molecule α-NTx-toxin inhibitors included the above controls, as well as α-BgTx controls of 30 nM (MIN) and 3 nM (MID). For all experiments with toxin-inhibitors, the concentrations of antagonist and ACh were kept consistent and co-incubated with varying concentrations of toxin-inhibitor. The data was then normalised to the mean ACh control (100% signal) and ACh + venom/toxin (0% signal) controls using equation (1) with venom/toxin-inhibitory activity represented by recovery towards the 100% ACh signal.

$$\%\ response = \frac{(Sample - 0\%\ signal)}{(100\%\ signal - 0\%\ signal)}\ x\ 100 \quad (1)$$

All experiments had 3-8 replicates per plate and were repeated on three separate plates using different cell passage numbers (4-12), and each repeat was carried out on a different day. Normalised data was combined across plates by calculating the mean of the replicates of each plate to give a single value for each plate (n = 1) and subsequently calculating the mean of these combined values. As experiments were repeated three times, all experiments had n = 3, and each data point was plotted as the mean ± SD. Plate uniformity studies were carried out as previously described [44], with assay quality measured using Z prime (Z') analysis with an

acceptance criterion of ≥ 0.4 [45]. Each data point across the three plates was plotted individually (rather than mean ± SD), so the variability of responses across the plate could be visualised. All data analysis, graph plotting, and application of non-linear regression equations (2) and (3) to fit curves were carried out using Prism 9 (GraphPad, San Diego, CA, USA).

The following non-linear regression equation was applied to fit a curve to concentration-response plots to generate EC_{50} values:

$$Y = Bottom + \frac{(Top - Bottom)}{1+10^{((LogEC_{50} - X)HillSlope)}} \quad (2)$$

The following non-linear regression equation was applied to fit a curve to concentration-inhibition plots to generate IC_{50} values:

$$Y = Bottom + \frac{(Top - Bottom)}{1+10^{((LogIC_{50} - X)HillSlope)}} \quad (3)$$

3. Results

3.1 nAChR agonists produce fluorescent responses in TE671 cells that are blocked by known nAChR antagonists

To determine whether our modifications to the previously described assay protocols produced consistent data, we validated the assay using several known nAChR agonists (ACh, nicotine, and epibatidine) and antagonists (snake venom Lc-α-NTxs and Sc-α-NTxs) of the muscle-type nAChR, alongside assay buffer alone (negative control). The incubation of TE671 cells with this negative control plus the membrane potential dye resulted in a slight decrease in the RFU readings that remained slightly below $F_{baseline}$ levels for the remainder of the recording, indicating that the addition of solution itself causes a small decrease in fluorescence (Fig. 1). The addition of the three nAChR agonists resulted in concentration-dependent increases in

fluorescence. The profile of the responses to all agonists typically reached F_{max} approximately 45 s after addition, followed by a slow decay for the remainder of the recording to up to 50% of the peak (Fig. 2A). Concentration-response curves revealed a rank order of potency of epibatidine > ACh > nicotine (Fig. 2B, Table 1). In the case of epibatidine, increasing agonist concentrations beyond 10 µM resulted in decreased responses indicating an agonist-dependent antagonism (Fig. 2B). ACh was chosen as the agonist for further experiments, as the activation of nAChRs by ACh is the most biologically relevant interaction for a snake toxin-inhibitor to restore. 10 µM ACh was chosen as the control concentration for further experiments, as it was the lowest concentration that produced the highest level of fluorescence (typically 150-250 RFUs), providing the largest signal window for further experiments, while avoiding an oversaturating concentration of ACh.

Next, we assessed the ability of the assay to detect nAChR antagonism by α-NTxs. Wang et al. [25] previously demonstrated antagonism by α-BgTx, a Lc-α-NTx isolated from the venom of *B. multicinctus*, to the nicotine response of TE671 cells using membrane potential dye [32]. Consequently, α-BgTx was used along with a commercially available Sc-α-NTx, namely sNTx1 from the venom of *N. pallida*, which was used in previous studies to investigate Sc-α-NTx activity on nAChRs under the name 'toxin α' and originally thought to be isolated from venom of *N. nigricollis* [46]. We observed concentration-dependent antagonism of the 10 µM ACh response with both α-NTxs (Fig. 2C and 2D), and α-BgTx was selected as the positive control for measuring the nAChR antagonism of neurotoxic snake venoms in downstream experiments due to its extensive prior characterisation [47].

3.2 Fluorescent responses show an acceptable level of plate uniformity for assay use in screening campaigns

With the long-term goal of applying our approach as a novel toxin-inhibitor screening assay, the following controls were selected to assess the uniformity of the assay; i) MAX, a maximal signal produced by 10 µM of the agonist ACh, ii) MIN, a minimal signal produced by the co-application of 10 µM ACh with 30 nM of the antagonist α-BgTx, and iii) MID, a medium signal using the co-application of 10 µM ACh with an IC_{50} concentration of the antagonist α-BgTx (3 nM). Using plates interleaved with these controls (a repeating pattern of three columns occupied by one of each of the controls), inter-day and intra-96 well plate uniformity of assays were performed following a previously described approach [44]. The inter-day assessments validated the reproducibility between different cell populations and passage numbers, whilst the intra-96 well plate experiments revealed no major edge or drift effects, which would invalidate the results when utilising all wells in the plates. Examination of the i) average F_{max}-$F_{baseline}$; ii) standard deviations (SD), and iii) coefficient of variations (CV) of the control signals showed clear separation in the three control signals within all plates (Fig. 3). In addition to the low CV and SD, these controls allowed for Z prime (Z') calculations [45], which are common practice in industrial scale drug screening programmes to determine the distribution of MIN/MAX signals and thus provide confidence that false positive or negative results will not occur. The Z prime of each plate (0.56, 0.62, and 0.57) surpassed the industry-accepted threshold of >0.4, as evidenced by the large signal window and small variance between the MAX and MIN readings.

To assess intra-plate uniformity for each of the three plates, the controls were plotted in spatial order, either by column (Fig. 3A) or row (Fig. 3B). This revealed no consistent drift or edge effects, either across the plate (Fig. 3A – by columns) or down the plate (Fig. 3B – by rows) for all plates. The resulting consistency confirms that responses remain consistent during the read time of the full plate of approximately 40 min where there is a time difference of more than 30 min between the reading of the first and last columns. This validation therefore provides

312 evidence for the use of all wells on the plate, thereby maximising the capacity for multi-plate
313 throughput in a screening campaign. However, inter-plate variation in RFU values after F_{max}-
314 $F_{baseline}$ calculation was observed, highlighting the need to normalise readings to the MAX
315 (100% response) and MIN (0% response) control signals to ensure robust cross-plate
316 comparisons. As the entire plate is not read at the same time and responses remain consistent
317 over the recording period, this approach allows the use of a less costly plate reader and is
318 therefore more accessible for many laboratories to implement.

319

320 **3.3 Neurotoxic snake venoms block the ACh response of TE671 cells**

321 Next, we used the developed assay to quantify nAChR antagonism by crude venoms
322 sourced from a variety of medically important African snake species. To this end, we selected
323 eight venoms from cobra (*Naja* spp.) and mamba (*Dendroaspis* spp.) species that are known to
324 contain high abundances of α-NTxs [48–50] and cause systemic neurotoxicity in snakebite
325 victims [11]. All venoms tested showed concentration-dependent antagonism of the TE671
326 ACh response after pre-incubation with the cells for 15 min (Fig. 4). However, we observed a
327 100-fold difference in potency across this group of related African elapid snakes (IC_{50}s range
328 from 0.03 – 4.49 µg/mL, Table 1, Fig. 4). Venom potency was seemingly not associated with
329 taxonomy, with the rank order of venom IC_{50} from most to least potent being *N. subfulva*, *D.*
330 *polylepis*, *D. j. kaimosae*, *D. j. jamesoni*, *N. nivea*, *N. haje*, *D. viridis,* and *D. angusticeps* (Fig.
331 4 and Table 1).

332

333 **3.4 Different formats of snake toxin-inhibiting molecules rescue the TE671 cell ACh**
334 **response**

In recent years, various molecules have been explored as potential new therapies for snake venom toxins (for a comprehensive overview, see [16,51]). To explore the utility of our assay as a functional screen to detect novel toxin-inhibitory molecules, we selected representatives of these different therapeutic formats (antivenoms, small molecule drugs, nAChR-mimicking proteins, and monoclonal antibodies) and assessed their ability to inhibit the nAChR antagonism stimulated by representative neurotoxic snake venoms (from *N. haje* and *D. polylepis*) and α-NTxs (α-BgTx and sNTx1). In line with the WHO guidelines for preclinical testing of antivenoms [13] and many other *in vitro* and *in vivo* approaches to assess venom inhibition [17,21,28,52], we performed these experiments with an initial pre-incubation step, where inhibitor and venom/toxin were co-incubated at 37 °C for 30 min before assaying, to give the inhibitor maximal opportunity to exhibit neutralisation (Fig. 5). To that end, we also performed these experiments with inhibitory molecules pre-incubated with the lowest venom or toxin concentrations that exhibited maximal nAChR antagonism (6.67 µg/mL for *N. haje* venom, 0.67 µg/mL for *D. polylepis* venom, and 30 nM for α-BgTx and sNTx1). This approach ensured the largest separation between agonist only (100%) and venom/toxin only (0%) signals and that there was not an oversaturating concentration of venom/toxin. In most cases, the inclusion of a 30 min pre-incubation step resulted in a modest increase in the venom/toxin only response (~10-15% of the agonist only response) (Fig. 5) compared to the response previously observed without incubation (<5%) (i.e., Figs. 2, 3 and 4).

3.4.1 Commercial antivenoms

Commercial polyclonal antibody-based antivenoms are currently the only available specific treatment for snakebite envenoming and are produced by immunising animals with sub-toxic doses of either a single or multiple venoms, resulting in monovalent or polyvalent antivenoms, respectively [13]. We assessed the capability of the assay to detect venom toxin inhibition using SAIMR polyvalent antivenom, which is manufactured using venoms from

multiple African cobra and mamba species in the immunisation mixture and, based on prior preclinical research, is known to inhibit venom neurotoxins [53–55]. We used the monovalent antivenom EchiTAbG as a control antivenom, and we did not anticipate observing venom inhibition with this product, as it is specific to the toxins found in the venom of the unrelated, non-neurotoxic, saw-scaled viper, *Echis ocellatus* [56]. Serial dilutions of each antivenom were co-incubated with *D. polylepis* and *N. haje* venom, and responses to ACh addition were compared with responses obtained with venom alone. As anticipated, SAIMR polyvalent antivenom demonstrated concentration-dependent inhibition against the nAChR antagonism caused by both snake venoms, while the non-specific control antivenom EchiTAbG did not show inhibitory activity at any of the concentrations tested (Fig. 5A). Interestingly, SAIMR polyvalent antivenom exhibited greater inhibition against *D. polylepis* venom than *N. haje* based on the lower EC_{50} value, equating to a mass ratio of 1:11.7 (venom:antivenom) against *D. polylepis* and 1:21.9 against *N. haje*, when accounting for differences in venom challenge doses. These findings indicate that more SAIMR polyvalent antivenom is required to neutralise the antagonism of *N. haje* venom, which might be explained by the presence of *D. polylepis*, but not *N. haje* venom in the immunising mixture used to generate this antivenom (instead venoms from related *Naja* spp. are used). Alternatively, the observed differences in neutralising potencies could be due to the considerably higher abundance of α-NTxs in *N. haje* venom [54,57].

3.4.2 Small molecule drug candidates

Next, a panel of small molecules that consisted of either a component from a plant extract that previously demonstrated neutralising activity [40] or that were identified through molecular docking studies of a chemical library with a Lc-α-NTx (α-BgTx or α-cobratoxin from *N. kaouthia*) [41,42] were investigated for their neurotoxin-inhibiting activity (Fig. 5B). Also included in the panel were known nAChR modulators and, as a control, varespladib which

is a small molecule inhibitor that exhibits potent inhibition of a different family of toxins found in snake venoms (PLA_2s), and which is in clinical development [20]. All small molecules were pre-incubated with venoms at a concentration of 100 µM, but only brucinic acid (NSC 121865) exhibited inhibitory activity. Further, inhibitory effects were only observed against *N. haje* venom, where the response was recovered to 41.3% of the control response (Fig. 5B). However, no α-NTx-inhibiting activity was observed for brucinic acid against *D. polylepis* venom.

3.4.3 nAChR-mimicking proteins

AChBPs are soluble proteins found in several mollusc species, and the variant found in *Lymnaea stagnalis* (*Ls*-AChBP) shares features with the human α7 nAChR [58]. A recent study showed that *Ls*-AChBP can bind Lc-α-NTxs from various crude snake venoms, and thus shows potential to act as a decoy molecule that can intercept toxins targeting nAChRs and prevent or delay neurotoxicity [17]. Considering this and previous data showing that Lc-α-NTxs possess a much higher affinity for the α7 nAChR than Sc-α-NTxs [46], we measured the ability of *Ls*-AChBP to inhibit the effects of α-BgTx and sNTx1 in the assay. α-NTxs were pre-incubated with serial dilutions of *Ls*-AChBP, and inhibition of α-BgTx activity was detected (Fig. 5C). Molar ratios were calculated based on an approximate molecular mass of 25 kDa for the *Ls*-AChBP monomer, and the highest molar ratio (α-BgTx:*Ls*-AChBP) of 1:156 restored activity to 86.0% of the ACh control. The lowest ratio to exhibit any restoration was 1:1.56 (16.2% of ACh control). As anticipated, we observed no inhibition of the antagonism of sNTx1 at any of the tested *Ls*-AChBP concentrations (Fig. 5C).

3.4.4 Monoclonal antibodies

A recent study identified the mAbs 2551_01_A12 and 2554_01_D11 as effective inhibitors of several Lc-α-NTxs, including α-BgTx, using automated patch-clamp electrophysiology and murine *in vivo* experimentation [21]. Consequently, we used our assay

409 to explore whether the α-NTx inhibition of these mAbs could also be detected in this assay,
410 using α-BgTx as our model (Fig. 5C). Pre-incubation of solutions containing 1:1.09, 1:2.19 and
411 1:4.37 molar ratios (α-BgTx:mAb), calculated based on using 150 kDa as an approximate
412 molecular mass for each IgG1 mAb, were tested, alongside a negative control mAb
413 (367_01_H01) directed against dendrotoxins from *D. polylepis* venom [59]. Concentration-
414 dependent inhibition of α-BgTx activity was observed with both antibodies directed against
415 Lc-α-NTxs (2551_01_A12 and 2554_01_D11), in line with previous electrophysiological
416 findings [21]. The mAb 2554_01_D11 was able to restore nAChR activity to a higher
417 percentage of ACh control (83.1%) than 2551_01_A12 (33.6%) at the highest dose tested. As
418 anticipated, the control anti-dendrotoxin mAb (367_01_H01) exhibited no inhibition of α-
419 BgTx antagonism of the nAChR, even at the highest concentrations tested.

420

421 **4. Discussion**

422 In this study, we developed a cell-based assay to investigate venom toxin activity on
423 muscle-type nAChR activation and explored its capability to detect inhibition by various toxin-
424 inhibiting molecules. For validation, we first quantified the effects of known nAChR agonists
425 and antagonists to ensure that their observed effects were consistent with other validated
426 experimental techniques, and that any modifications made to previously published approaches
427 [31,32] did not affect the assay (Fig. 2). The time to peak and decay of fluorescent responses
428 during the recording time (Fig. 2A) were consistent to those observed in other studies
429 employing the same experimental approach [60], though differences were observed when
430 comparing outcomes with electrophysiology approaches. Responses of muscle-type nAChRs
431 typically reach a peak and return to baseline within a few seconds in electrophysiology
432 experiments [61], while the responses observed in this assay do not return to baseline after 214

s of recording (Fig. 2A and 2C). This prolonged response could perhaps be due to a positive allosteric modulatory effect of the dye or the activation of natively expressed voltage-gated ion channels [43] after nAChR activation. Irrespectively, the profile of responses and the sensitivity of the assay to traditional nAChR modulators confirms the utility of this approach for measuring nAChR activation, rather than other physiological properties of the channel. The EC_{50}s for agonists (Table 1) also differ from those obtained with electrophysiology approaches [33,62–64], but remain consistent with those obtained in previous studies using the same experimental approach [31,37]. Antagonism by α-BgTx was confirmed as in previous studies (Fig. 2C and 2D) [32,65], and sNTx1 also exhibited antagonism (Fig. 2C and 2D), which was anticipated given that binding of this α-NTx to the muscle-type nAChR has previously been demonstrated [46]. Collectively, these data provide confidence that the developed assay is informative for assessing nAChR agonism and antagonism.

All snake venoms tested in this study (from *Naja* and *Dendroaspis* spp.) showed evidence of antagonism on the muscle-type nAChR (Fig. 4). These findings were anticipated, since: (i) systemic envenoming by these species result in neurotoxic clinical manifestations in snakebite patients [11,12], (ii) α-NTxs have previously been identified in various mamba and cobra venoms [48–50,54,55], and (iii) venoms from *N. haje* and *D. polylepis* have previously been demonstrated to exhibit nAChR antagonism in functional assays [32,66]. Since there was an almost 100-fold difference in potency of the crude neurotoxic venoms investigated in this study, with no obvious correlation with taxonomy, investigation of additional elapid venoms from diverse genera could be particularly revealing to unravel the evolutionary basis of these considerable differences in venom potency. Given the medical importance of α-NTxs, the assay described here could be readily used in conjunction with venom fractionation/purification and identification approaches [55,67] to identify the key α-NTxs responsible for nAChR-mediated neurotoxicity. Such 'toxicovenomic' profiling is important, as each snake venom can

potentially contain multiple α-NTxs, and these likely differ in both potency and abundance, as well as they may vary both intra- and inter-specifically [49,54,68]. The identification of such toxins is important for the rational selection of targets for novel therapeutics (antivenoms and toxin-inhibitory molecules), and/or to either supplement or use as alternatives to, whole venoms as immunogens for antivenom production [18,69]. Additionally, given that toxins outside of the 3FTx family have also been demonstrated to exert nAChR antagonism [70], this approach may also prove useful for identifying novel venom neurotoxins.

The assay was further demonstrated to be compatible with the detection of ability of various therapeutic candidate molecules to inhibit the antagonism of venom neurotoxins on the nAChR (Fig. 5). In several cases, pre-incubation with venom or α-NTxs resulted in a restoration to >80% of the control response, demonstrating clear inhibition (e.g., SAIMR polyvalent antivenom, *Ls*-AChBP, and mAb 2554_01_D11). Given the demonstrated acceptable level of uniformity across a 96-well plate (Fig. 3), there is clear potential to use this assay as a screening platform for the identification of novel toxin-inhibiting molecules against venom nAChR-antagonists. For example, in an approach analogous to that proposed elsewhere for other venom toxins [71], this assay could be implemented as a primary drug screening assay to identify α-NTx-inhibiting molecules present in compound libraries consisting of drugs that are already approved or in development for other indications. This 'drug repurposing' approach is particularly attractive for snakebite envenoming, as ensuing hits have often entered at least early-stage clinical trials for other indications, resulting in potentially shorter development timelines compared with the development of new chemical entities, and therefore potentially lower development costs [71]. Similarly, this assay could be used for aiding the discovery and optimisation of cross-reactive mAbs directed against α-NTxs and other 3FTxs. Such approaches currently rely on binding assays for screening [72], typically followed by complex and expensive bioassays (e.g., patch-clamp electrophysiology or *in vivo* preclinical studies) to

assess α-NTx inhibition [21]. The same principles apply to the development of receptor-mimicking peptides/proteins based around AChBP scaffolds. Recent insights into the properties of Sc-α-NTx binding to muscle-type nAChRs [61] should aid the future protein engineering of AChBP derivatives and receptor-mimicking peptides designed to simultaneously capture both Lc-α-NTxs and Sc-α-NTxs. Such molecules could be readily screened in this assay for their generic α-NTx-inhibiting activity as an initial readout to inform downstream structural optimisation and lead candidate selection.

The use of the human muscle-type nAChR in this assay is a particular strength, as questions have been raised about the appropriateness of rodent models for assessing the activity of α-NTxs due to Sc-α-NTxs exhibiting enhanced potency on rodent nAChRs [73]. Investigating human nAChRs in TE671 cells can help ensure that only toxins relevant to causing neurotoxicity in snakebite victims are being studied. However, certain α-NTxs can exhibit enhanced potency for foetal (γ subunit-containing) muscle-type nAChRs (subtype expressed in TE671 cells) over the adult (ε subunit-containing) type, as previously observed with the Sc-α-NTx 'NmmI' from *N. mossambica* [74]. The CN21 cell line, used in a similar cell-based fluorescence assay to investigate chemicals to counteract organophosphate poisoning [75], expresses the adult muscle-type nAChR and could be employed in place of TE671 cells to distinguish α-NTxs selective for foetal muscle-type nAChRs. Another future expansion of this assay would be to employ a more challenging model of envenoming. After identifying promising α-NTx-inhibiting candidates in pre-incubation experiments, these candidates could then be assessed using a model where venom/toxin is applied simultaneously or before the toxin-inhibitor. This is relevant, because a major hurdle for α-NTx treatments to overcome is the long dissociation time of Lc-α-NTxs once bound to the nAChR [68]. Studies using chick biventer cervicis nerve-muscle preparations and commercial antivenoms have employed an analogous approach and showed the ability of antivenoms to reverse α-NTx dependent

508 inhibition of nAChRs when applied after treatment with Asian cobra venoms [76] and
509 *Oxyuranus scutellatus* venom [77]. Adaptation of our assay in a similar manner could allow
510 for further discrimination between inhibitors that promote toxin dissociation from the nAChR
511 compared with those that need to intercept α-NTxs before they bind.

512 The herein described approach of measuring TE671 cell muscle-type nAChR activation
513 using membrane potential dye has enabled the assessment of nAChR antagonism by crude
514 elapid snake venoms and isolated Lc-α-NTx and Sc-α-NTxs. As both classes of α-NTxs
515 exhibited dose-dependent antagonism, the assay provides a robust platform to investigate
516 toxicity mediated by α-NTxs from the venoms of snake species found across different
517 geographical regions. This assay could also find wider utility for studying nAChR modulators,
518 whether from natural (e.g., other animal venoms or toxins) or chemical sources. In addition,
519 we demonstrated the utility of the assay for identifying α-NTx-inhibitory molecules and
520 highlight its compatibility with four major categories of snakebite therapeutics currently being
521 explored. We therefore hope that this assay will be a useful addition to the experimental toolbox
522 to identify new therapeutics against key neurotoxins from snake venoms, and that it will help
523 deliver new toxin-inhibitors that can mitigate the many life-threatening snakebite envenomings
524 that occur worldwide each year.

525

526 **Acknowledgments**

527 We thank David Richards for early discussions on the assay concept, Ian Mellor
528 (University of Nottingham, UK) for the gift of TE671 cells, and IONTAS (Cambridge, UK)
529 for facilitating access to the monoclonal antibodies. We also thank Jory van Thiel for the
530 creation of species distribution maps presented in Fig. 4, Paul Rowley and Edouard Crittenden
531 (Liverpool School of Tropical Medicine, UK) for expert maintenance of venomous snakes and

provision of venom samples, as well as use of photographs presented in Fig, 4, alongside those generously provided by Taline Kazandjian, Steven Hall, Simon Townsley, and Wolfgang Wüster. This work was supported by the Wellcome Trust funded project grants 221710/Z/20/Z (CU, JK and NRC) and 221712/Z/20/Z (NRC and JK) and KU Leuven grant C32/16/035 (CU). MN is a recipient of a FWO postdoctoral fellowship 12X2722N. This research was funded in part by the Wellcome Trust. For the purpose of open access, the authors have applied a CC BY public copyright licence to any Author Accepted Manuscript version arising from this submission.

References

[1] A. Kasturiratne, A.R. Wickremasinghe, N. de Silva, N.K. Gunawardena, A. Pathmeswaran, R. Premaratna, L. Savioli, D.G. Lalloo, H.J. de Silva, The Global Burden of Snakebite: A Literature Analysis and Modelling Based on Regional Estimates of Envenoming and Deaths, PLoS Med. 5 (2008) e218.

[2] D.J. Williams, M.A. Faiz, B. Abela-Ridder, S. Ainsworth, T.C. Bulfone, A.D. Nickerson, A.G. Habib, T. Junghanss, H.W. Fan, M. Turner, R.A. Harrison, D.A. Warrell, Strategy for a globally coordinated response to a priority neglected tropical disease: Snakebite envenoming, PLoS Negl Trop Dis. 13 (2019) e0007059.

[3] N.R. Casewell, T.N.W. Jackson, A.H. Laustsen, K. Sunagar, Causes and Consequences of Snake Venom Variation, Trends Pharmacol Sci. 41 (2020) 570–581.

[4] C.R. Ferraz, A. Arrahman, C. Xie, N.R. Casewell, R.J. Lewis, J. Kool, F.C. Cardoso, Multifunctional Toxins in Snake Venoms and Therapeutic Implications: From Pain to Hemorrhage and Necrosis, Front Ecol Evol. 7 (2019) 1–19.

[5] T. Tasoulis, G.K. Isbister, A review and database of snake venom proteomes, Toxins (Basel). 9 (2017) 1–23.

[6] S. Nirthanan, Snake three-finger α-neurotoxins and nicotinic acetylcholine receptors: molecules, mechanisms and medicine, Biochem Pharmacol. 181 (2020) 114168.

[7] V.I. Tsetlin, I.E. Kasheverov, Y.N. Utkin, Three-finger proteins from snakes and humans acting on nicotinic receptors: Old and new, J Neurochem. 158 (2021) 1223–1235.

[8] E.X. Albuquerque, E.F.R. Pereira, M. Alkondon, S.W. Rogers, Mammalian nicotinic acetylcholine receptors: From structure to function, Physiol Rev. 89 (2009) 73–120.

563 [9] H. Cetin, D. Beeson, A. Vincent, R. Webster, The Structure, Function, and Physiology
564 of the Fetal and Adult Acetylcholine Receptor in Muscle, Front Mol Neurosci. 13 (2020)
565 170.

566 [10] C.M. Barber, G.K. Isbister, W.C. Hodgson, Alpha neurotoxins, Toxicon. 66 (2013) 47–
567 58.

568 [11] U.K. Ranawaka, D.G. Lalloo, H.J. de Silva, Neurotoxicity in Snakebite-The Limits of
569 Our Knowledge, PLoS Negl Trop Dis. 7 (2013) e2302.

570 [12] P.E. Bickler, M. Abouyannis, A. Bhalla, M.R. Lewin, Neuromuscular Weakness and
571 Paralysis Produced by Snakebite Envenoming: Mechanisms and Proposed Standards for
572 Clinical Assessment, Toxins (Basel). 15 (2023) 49.

573 [13] World Health Organization, Guidelines for the production, control and regulation of
574 nake antivenom immunoglobulins, Annex 5, TRS No 1004, 2013.

575 [14] World Health Organization, Guidelines for the management of snakebites, 2nd edition,
576 (2016). https://www.who.int/publications/i/item/9789290225300 (accessed November
577 11, 2022).

578 [15] J. Potet, D. Beran, N. Ray, G. Alcoba, A.G. Habib, G. Iliyasu, B. Waldmann, R. Ralph,
579 M.A. Faiz, W.M. Monteiro, J. de Almeida Gonçalves Sachett, J.L. di Fabio, M. de los
580 Á. Cortés, N.I. Brown, D.J. Williams, Access to antivenoms in the developing world: A
581 multidisciplinary analysis, Toxicon X. 12 (2021) 100086.

582 [16] A. Laustsen, M. Engmark, C. Milbo, J. Johannesen, B. Lomonte, J. Gutiérrez, B. Lohse,
583 From Fangs to Pharmacology: The Future of Snakebite Envenoming Therapy, Curr
584 Pharm Des. 22 (2016) 5270–5293.

585 [17] L.O. Albulescu, T. Kazandjian, J. Slagboom, B. Bruyneel, S. Ainsworth, J. Alsolaiss,
586 S.C. Wagstaff, G. Whiteley, R.A. Harrison, C. Ulens, J. Kool, N.R. Casewell, A decoy-
587 receptor approach using nicotinic acetylcholine receptor mimics reveals their potential
588 as novel therapeutics against neurotoxic snakebite, Front Pharmacol. 10 (2019) 1–15.

589 [18] G. de la Rosa, F. Olvera, I.G. Archundia, B. Lomonte, A. Alagón, G. Corzo, Horse
590 immunization with short-chain consensus α-neurotoxin generates antibodies against
591 broad spectrum of elapid venomous species, Nat Commun. 10 (2019) 3642.

592 [19] L.O. Albulescu, C. Xie, S. Ainsworth, J. Alsolaiss, E. Crittenden, C.A. Dawson, R.
593 Softley, K.E. Bartlett, R.A. Harrison, J. Kool, N.R. Casewell, A therapeutic combination
594 of two small molecule toxin inhibitors provides broad preclinical efficacy against viper
595 snakebite, Nat Commun. 11 (2020) 6094.

596 [20] M. Lewin, S. Samuel, J. Merkel, P. Bickler, Varespladib (LY315920) Appears to Be a
597 Potent, Broad-Spectrum, Inhibitor of Snake Venom Phospholipase A_2 and a Possible
598 Pre-Referral Treatment for Envenomation, Toxins (Basel). 8 (2016) 248.

599 [21] L. Ledsgaard, J. Wade, T.P. Jenkins, K. Boddum, I. Oganesyan, J.A. Harrison, P. Villar,
600 R.A. Leah, R. Zenobi, S. Schoffelen, B. Voldborg, A. Ljungars, J. McCafferty, B.
601 Lomonte, J.M. Gutiérrez, A.H. Laustsen, A. Karatt-Vellatt, Discovery and optimization

602 of a broadly-neutralizing human monoclonal antibody against long-chain α-neurotoxins
603 from snakes, Nat Commun 14 (2023) 1–14.

604 [22] T. Lynagh, S. Kiontke, M. Meyhoff-Madsen, B.H. Gless, J. Johannesen, S. Kattelmann,
605 A. Christiansen, M. Dufva, A.H. Laustsen, K. Devkota, C.A. Olsen, D. Kümmel, S.A.
606 Pless, B. Lohse, Peptide Inhibitors of the α-Cobratoxin-Nicotinic Acetylcholine
607 Receptor Interaction, J Med Chem. 63 (2020) 13709–13718.

608 [23] B.G. Fry, Venomous Reptiles and Their Toxins: Evolution, Pathophysiology and
609 Biodiscovery, Oxford University Press, 2015.

610 [24] L. Ledsgaard, A.H. Laustsen, U. Pus, J. Wade, P. Villar, K. Boddum, P. Slavny, E.W.
611 Masters, A.S. Arias, S. Oscoz, D.T. Griffiths, A.M. Luther, M. Lindholm, R.A. Leah,
612 M.S. Møller, H. Ali, J. McCafferty, B. Lomonte, J.M. Gutiérrez, A. Karatt-Vellatt, *In*
613 *vitro* discovery of a human monoclonal antibody that neutralizes lethality of cobra snake
614 venom, MAbs. 14 (2022) 2085536.

615 [25] S. Miersch, G. de la Rosa, R. Friis, L. Ledsgaard, K. Boddum, A.H. Laustsen, S.S. Sidhu,
616 Synthetic antibodies block receptor binding and current-inhibiting effects of α-
617 cobratoxin from *Naja kaouthia*, Protein Science. 31 (2022) e4296.

618 [26] J. Wade, C. Rimbault, H. Ali, L. Ledsgaard, E. Rivera-De-Torre, M. Abou Hachem, K.
619 Boddum, N. Mirza, M.F. Bohn, S.A. Sakya, F. Ruso-Julve, J.T. Andersen, A.H.
620 Laustsen, Generation of Multivalent Nanobody-Based Proteins with Improved
621 Neutralization of Long α-Neurotoxins from Elapid Snakes, Bioconjug Chem. 33 (2022)
622 1494–1504.

623 [27] C.N. Zdenek, R.J. Harris, S. Kuruppu, N.J. Youngman, J.S. Dobson, J. Debono, M.
624 Khan, I. Smith, M. Yarski, D. Harrich, C. Sweeney, N. Dunstan, L. Allen, B.G. Fry, A
625 Taxon-Specific and High-Throughput Method for Measuring Ligand Binding to
626 Nicotinic Acetylcholine Receptors, Toxins (Basel). 11 (2019) 600.

627 [28] K. Pruksaphon, K.Y. Tanid, C.H. Tan, P. Simsiriwong, J.M. Gutiérrezid, K.
628 Ratanabanangkoonid, An *in vitro* α-neurotoxin—nAChR binding assay correlates with
629 lethality and *in vivo* neutralization of a large number of elapid neurotoxic snake venoms
630 from four continents, PLoS Negl Trop Dis. 14 (2020) e0008581.

631 [29] J. Slagboom, R.A. Otvos, F.C. Cardoso, J. Iyer, J.C. Visser, B.R. van Doodewaerd,
632 R.J.R. McCleary, W.M.A. Niessen, G.W. Somsen, R.J. Lewis, R.M. Kini, A.B. Smit,
633 N.R. Casewell, J. Kool, Neurotoxicity fingerprinting of venoms using on-line
634 microfluidic AChBP profiling, Toxicon. 148 (2018) 213–222.

635 [30] M.A. Luther, R. Schoepfer, P. Whiting, B. Casey, Y. Blatt, M.S. Montal, M. Montal, J.
636 Lindstrom, A muscle acetylcholine receptor is expressed in the human cerebellar
637 medulloblastoma cell line TE671, Journal of Neuroscience. 9 (1989) 1082–1096.

638 [31] R.W. Fitch, Y. Xiao, K.J. Kellar, J.W. Daly, Membrane potential fluorescence: A rapid
639 and highly sensitive assay for nicotinic receptor channel function, Proc Natl Acad Sci U
640 S A. 100 (2003) 4909–4914.

641 [32] C.-I.A. Wang, T. Reeks, I. Vetter, I. Vergara, O. Kovtun, R.J. Lewis, P.F. Alewood, T.
642 Durek, Isolation and Structural and Pharmacological Characterization of α-Elapitoxin-

643 Dpp2d, an Amidated Three Finger Toxin from Black Mamba Venom, Biochemistry. 53
644 (2014) 3758–3766.

645 [33] R.N. Patel, D.P. Richards, I.R. Duce, M.A. Birkett, D.B. Sattelle, I.R. Mellor, Actions
646 on mammalian and insect nicotinic acetylcholine receptors of harmonine-containing
647 alkaloid extracts from the harlequin ladybird *Harmonia axyridis*, Pestic Biochem
648 Physiol. 166 (2020) 104561.

649 [34] H. Rollema, L.K. Chambers, J.W. Coe, J. Glowa, R.S. Hurst, L.A. Lebel, Y. Lu, R.S.
650 Mansbach, R.J. Mather, C.C. Rovetti, S.B. Sands, E. Schaeffer, D.W. Schulz, F.D.
651 Tingley, K.E. Williams, Pharmacological profile of the α4β2 nicotinic acetylcholine
652 receptor partial agonist varenicline, an effective smoking cessation aid,
653 Neuropharmacology. 52 (2007) 985–994.

654 [35] G.S. Taiwe, J. Montnach, S. Nicolas, S. de Waard, E. Fiore, E. Peyrin, T.M.A. El-Aziz,
655 M. Amar, J. Molgó, M. Ronjat, D. Servent, C. Ravelet, M. de Waard, Aptamer Efficacies
656 for *In Vitro* and *In Vivo* Modulation of αC-Conotoxin PrXA Pharmacology, Molecules
657 2019, Vol. 24, Page 229. 24 (2019) 229.

658 [36] R.L. Leong, H. Xing, J.-C. Braekman, W.R. Kem, Non-competitive Inhibition of
659 Nicotinic Acetylcholine Receptors by Ladybird Beetle Alkaloids, Neurochem Res. 40
660 (2015) 2078–2086.

661 [37] B.T. Green, K.D. Welch, D. Cook, D.R. Gardner, Potentiation of the actions of
662 acetylcholine, epibatidine, and nicotine by methyllycaconitine at fetal muscle-type
663 nicotinic acetylcholine receptors, Eur J Pharmacol. 662 (2011) 15–21.

664 [38] S.T. Lee, K. Wildeboer, K.E. Panter, W.R. Kem, D.R. Gardner, R.J. Molyneux, C.W.T.
665 Chang, F. Soti, J.A. Pfister, Relative toxicities and neuromuscular nicotinic receptor
666 agonistic potencies of anabasine enantiomers and anabaseine, Neurotoxicol Teratol. 28
667 (2006) 220–228.

668 [39] M. Kassner, J.B. Eaton, N. Tang, J.L. Petit, N. Meurice, H.H. Yin, P. Whiteaker, High-
669 throughput cell-based assays for identifying antagonists of multiple smoking-associated
670 human nicotinic acetylcholine receptor subtypes, SLAS Discov. 27 (2022) 68–76.

671 [40] T. Sivaraman, N.S. Sreedevi, S. Meenachisundharam, R. Vadivelan, Neutralizing
672 potential of *Rauvolfia serpentina* root extract against *Naja naja* venom, Brazilian
673 Journal of Pharmaceutical Sciences. 56 (2020) 1–10.

674 [41] M. Utsintong, T.T. Talley, P.W. Taylor, A.J. Olson, O. Vajragupta, Virtual screening
675 against alpha-cobratoxin, J Biomol Screen. 14 (2009) 1109–1118.

676 [42] B.K. Rajendran, M. Xavier Suresh, S.P. Bhaskaran, Y. Harshitha, U. Gaur, H.F. Kwok,
677 Pharmacoinformatic Approach to Explore the Antidote Potential of Phytochemicals on
678 Bungarotoxin from Indian Krait, *Bungarus caeruleus*, Comput Struct Biotechnol J. 16
679 (2018) 450–461.

680 [43] N.M. Ngum, M.Y.A. Aziz, L. Mohammed Latif, R.J. Wall, I.R. Duce, I.R. Mellor, Non-
681 canonical endogenous expression of voltage-gated sodium channel NaV1.7 subtype by
682 the TE671 rhabdomyosarcoma cell line, J Physiol. 600 (2022) 2499–2513.

683 [44] P.W. Iversen, B. Beck, Y.-F. Chen, W. Dere, V. Devanarayan, B.J. Eastwood, M.W.
684 Farmen, S.J. Iturria, C. Montrose, R.A. Moore, J.R. Weidner, G.S. Sittampalam, HTS
685 Assay Validation, (2012). https://www.ncbi.nlm.nih.gov/books/ (accessed November 2,
686 2022).

687 [45] J.H. Zhang, T.D.Y. Chung, K.R. Oldenburg, A Simple Statistical Parameter for Use in
688 Evaluation and Validation of High Throughput Screening Assays, J Biomol Screen. 4
689 (1999) 67–73.

690 [46] D. Servent, V. Winckler-Dietrich, H.Y. Hu, P. Kessler, P. Drevet, D. Bertrand, A.
691 Ménez, Only snake curaremimetic toxins with a fifth disulfide bond have high affinity
692 for the neuronal alpha7 nicotinic receptor, J Biol Chem. 272 (1997) 24279–24286.

693 [47] M.M. Rahman, J. Teng, B.T. Worrell, C.M. Noviello, M. Lee, A. Karlin, M.H.B.
694 Stowell, R.E. Hibbs, Structure of the Native Muscle-type Nicotinic Receptor and
695 Inhibition by Snake Venom Toxins, Neuron. 106 (2020) 952-962.e5.

696 [48] T.D. Kazandjian, D. Petras, S.D. Robinson, J. van Thiel, H.W. Greene, K. Arbuckle, A.
697 Barlow, D.A. Carter, R.M. Wouters, G. Whiteley, S.C. Wagstaff, A.S. Arias, L.O.
698 Albulescu, A. Plettenberg Laing, C. Hall, A. Heap, S. Penrhyn-Lowe, C. V. McCabe, S.
699 Ainsworth, R.R. da Silva, P.C. Dorrestein, M.K. Richardson, J.M. Gutiérrez, J.J.
700 Calvete, R.A. Harrison, I. Vetter, E.A.B. Undheim, W. Wüster, N.R. Casewell,
701 Convergent evolution of pain-inducing defensive venom components in spitting cobras,
702 Science. 371 (2021) 386–390.

703 [49] S. Ainsworth, D. Petras, M. Engmark, R.D. Süssmuth, G. Whiteley, L.O. Albulescu,
704 T.D. Kazandjian, S.C. Wagstaff, P. Rowley, W. Wüster, P.C. Dorrestein, A.S. Arias,
705 J.M. Gutiérrez, R.A. Harrison, N.R. Casewell, J.J. Calvete, The medical threat of mamba
706 envenoming in sub-Saharan Africa revealed by genus-wide analysis of venom
707 composition, toxicity and antivenomics profiling of available antivenoms, J Proteomics.
708 172 (2018) 173–189.

709 [50] G.T.T. Nguyen, C. O'Brien, Y. Wouters, L. Seneci, A. Gallissà-Calzado, I. Campos-
710 Pinto, S. Ahmadi, A.H. Laustsen, A. Ljungars, High-throughput proteomics and *in vitro*
711 functional characterization of the 26 medically most important elapids and vipers from
712 sub-Saharan Africa, Gigascience. 11 (2022) 1–15.

713 [51] C. Knudsen, A.H. Laustsen, Recent Advances in Next Generation Snakebite
714 Antivenoms, Tropical Medicine and Infectious Disease 2018, 3 (2018) 42.

715 [52] J.M. Gutiérrez, B. Lomonte, L. Sanz, J.J. Calvete, D. Pla, Immunological profile of
716 antivenoms: Preclinical analysis of the efficacy of a polyspecific antivenom through
717 antivenomics and neutralization assays, J Proteomics. 105 (2014) 340–350.

718 [53] S. Ainsworth, S.K. Menzies, N.R. Casewell, R.A. Harrison, An analysis of preclinical
719 efficacy testing of antivenoms for sub-Saharan Africa: Inadequate independent scrutiny
720 and poor-quality reporting are barriers to improving snakebite treatment and
721 management, PLoS Negl Trop Dis. 14 (2020) e0008579.

722 [54] A.H. Laustsen, B. Lomonte, B. Lohse, J. Fernández, J.M. Gutiérrez, Unveiling the
723 nature of black mamba (*Dendroaspis polylepis*) venom through venomics and

antivenom immunoprofiling: Identification of key toxin targets for antivenom development, J Proteomics. 119 (2015) 126–142.

[55] L.P. Lauridsen, A.H. Laustsen, B. Lomonte, J.M. Gutiérrez, Toxicovenomics and antivenom profiling of the Eastern green mamba snake (*Dendroaspis angusticeps*), J Proteomics. 136 (2016) 248–261.

[56] N.R. Casewell, D.A.N. Cook, S.C. Wagstaff, A. Nasidi, N. Durfa, W. Wüster, R.A. Harrison, Pre-Clinical Assays Predict Pan-African *Echis* Viper Efficacy for a Species-Specific Antivenom, PLoS Negl Trop Dis. 4 (2010) e851.

[57] B.F. Hempel, M. Damm, D. Petras, T.D. Kazandjian, C.A. Szentiks, G. Fritsch, G. Nebrich, N.R. Casewell, O. Klein, R.D. Süssmuth, Spatial Venomics─Cobra Venom System Reveals Spatial Differentiation of Snake Toxins by Mass Spectrometry Imaging, J Proteome Res. 22 (2023) 26–35.

[58] A.B. Smit, N.I. Syed, D. Schaap, J. van Minnen, J. Klumperman, K.S. Kits, H. Lodder, R.C. van der Schors, R. van Elk, B. Sorgedrager, K. Brejc, T.K. Sixma, W.P.M. Geraerts, A glia-derived acetylcholine-binding protein that modulates synaptic transmission, Nature. 411 (2001) 261–268.

[59] A.H. Laustsen, A. Karatt-Vellatt, E.W. Masters, A.S. Arias, U. Pus, C. Knudsen, S. Oscoz, P. Slavny, D.T. Griffiths, A.M. Luther, R.A. Leah, M. Lindholm, B. Lomonte, J.M. Gutiérrez, J. McCafferty, *In vivo* neutralization of dendrotoxin-mediated neurotoxicity of black mamba venom by oligoclonal human IgG antibodies, Nat Commun. 9 (2018) 3928.

[60] B.T. Green, S.T. Lee, K.D. Welch, J.A. Pfister, K.E. Panter, Fetal muscle-type nicotinic acetylcholine receptor activation in TE-671 cells and inhibition of fetal movement in a day 40 pregnant goat model by optical isomers of the piperidine alkaloid coniine, J Pharmacol Exp Ther. 344 (2013) 295–307.

[61] M. Nys, E. Zarkadas, M. Brams, A. Mehregan, K. Kambara, J. Kool, N.R. Casewell, D. Bertrand, J.E. Baenziger, H. Nury, C. Ulens, The molecular mechanism of snake short-chain α-neurotoxin binding to muscle-type nicotinic acetylcholine receptors, Nat Commun. 13 (2022) 1–12.

[62] R.B. Jacobsen, RD(TE671)nAChR α1 on QPatch, Sophion Bioscience. (2010). https://sophion.com/publications/te671-nachr-a1-qpatch/ (accessed November 11, 2022).

[63] G. Gisselmann, D. Alisch, B. Welbers-Joop, H. Hatt, Effects of quinine, quinidine and chloroquine on human muscle nicotinic acetylcholine receptors, Front Pharmacol. 9 (2018) 1339.

[64] V. Gerzanich, X. Peng, F. Wang, G. Wells, R. Anand, S. Fletcher, J. Lindstrom, Comparative pharmacology of epibatidine: a potent agonist for neuronal nicotinic acetylcholine receptors, Mol Pharmacol. 48 (1995) 774-782.

[65] P.J. Syapin, P.M. Salvaterra, J.K. Engelhardt, Neuronal-like features of TE671 cells: Presence of a functional nicotinic cholinergic receptor, Brain Res. 231 (1982) 365–377.

764 [66] B. Hue, S.D. Buckingham, D. Buckingham, D.B. Sattelle, Actions of snake neurotoxins
765 on an insect nicotinic cholinergic synapse, Invertebrate Neuroscience. 7 (2007) 173–
766 178.

767 [67] J. Slagboom, R.J.E. Derks, R. Sadighi, G.W. Somsen, C. Ulens, N.R. Casewell, J. Kool,
768 High-Throughput Venomics, J Proteome Res. In press (2023). doi:
769 10.1021/acs.jproteome.2c00780.

770 [68] A. Silva, B. Cristofori-Armstrong, L.D. Rash, W.C. Hodgson, G.K. Isbister, Defining
771 the role of post-synaptic α-neurotoxins in paralysis due to snake envenoming in humans,
772 Cellular and Molecular Life Sciences. 75 (2018) 4465–4478.

773 [69] K. Ratanabanangkoon, K.Y. Tan, S. Eursakun, C.H. Tan, P. Simsiriwong, T.
774 Pamornsakda, W. Wiriyarat, C. Klinpayom, N.H. Tan, A Simple and Novel Strategy for
775 the Production of a Pan-specific Antiserum against Elapid Snakes of Asia, PLoS Negl
776 Trop Dis. 10 (2016) e0004565.

777 [70] C.A. Vulfius, E.N. Spirova, M. v. Serebryakova, I. v. Shelukhina, D.S. Kudryavtsev, E.
778 v. Kryukova, V.G. Starkov, N. v. Kopylova, M.N. Zhmak, I.A. Ivanov, K.S.
779 Kudryashova, T. v. Andreeva, V.I. Tsetlin, Y.N. Utkin, Peptides from puff adder *Bitis*
780 *arietans* venom, novel inhibitors of nicotinic acetylcholine receptors, Toxicon. 121
781 (2016) 70–76.

782 [71] R.H. Clare, S.R. Hall, R.N. Patel, N.R. Casewell, Small Molecule Drug Discovery for
783 Neglected Tropical Snakebite, Trends Pharmacol Sci. 42 (2021) 340–353.

784 [72] L. Ledsgaard, T.P. Jenkins, K. Davidsen, K.E. Krause, A. Martos-Esteban, M. Engmark,
785 M.R. Andersen, O. Lund, A.H. Laustsen, Antibody Cross-Reactivity in Antivenom
786 Research, Toxins (Basel). 10 (2018) 393.

787 [73] A. Silva, W.C. Hodgson, T. Tasoulis, G.K. Isbister, Rodent Lethality Models Are
788 Problematic for Evaluating Antivenoms for Human Envenoming, Front Pharmacol. 13
789 (2022) 202.

790 [74] H. Osaka, S. Malany, J.R. Kanter, S.M. Sine, P. Taylor, Subunit interface selectivity of
791 the alpha-neurotoxins for the nicotinic acetylcholine receptor, J Biol Chem. 274 (1999)
792 9581–9586.

793 [75] A. Ring, B.O. Strom, S.R. Turner, C.M. Timperley, M. Bird, A.C. Green, J.E. Chad, F.
794 Worek, J.E.H. Tattersall, Bispyridinium compounds inhibit both muscle and neuronal
795 nicotinic acetylcholine receptors in human cell lines, PLoS One. 10 (2015) e0135811.

796 [76] T.M. Huynh, W.C. Hodgson, G.K. Isbister, A. Silva, The Effect of Australian and Asian
797 Commercial Antivenoms in Reversing the Post-Synaptic Neurotoxicity of *O. hannah*,
798 *N. naja* and *N. kaouthia* Venoms *In Vitro*, Toxins. 14 (2022) 277.

799 [77] U. Madhushani, G.K. Isbister, T. Tasoulis, W.C. Hodgson, A. Silva, *In-Vitro*
800 Neutralization of the Neurotoxicity of Coastal Taipan Venom by Australian Polyvalent
801 Antivenom: The Window of Opportunity, Toxins. 12 (2020) 690.

802

803

804 **Table 1. The EC_{50} and IC_{50} values of known nAChR agonists, isolated snake venom α-**
805 **NTxs, and crude snake venoms obtained in this study**

nAChR modulator		
	EC_{50} (μM)	***95% CI (μM)***
Agonist		
Acetylcholine (ACh)	0.95	0.86 – 1.05
Nicotine	34.00	26.60 – 43.40
Epibatidine	0.08	0.03 – 0.23
Isolated venom toxins	***IC_{50} (nM)***	***95% CI (nM)***
α-Bungarotoxin (α-BgTx)	1.42	0.83 – 2.44
Short neurotoxin 1 (sNTx1)	7.23	4.83 – 10.80
Crude snake venom	***IC_{50} (μg/mL)***	***95% CI (μg/mL)***
Dendroaspis polylepis	0.04	0.02 – 0.06
Dendroaspis j. kaimosae	0.10	0.04 – 0.29
Dendroaspis j. jamesoni	0.14	0.08 – 0.25
Dendroaspis viridis	0.59	0.22 – 1.37
Dendroaspis angusticeps	4.49	2.24 – 9.02
Naja subfulva	0.03	0.02 – 0.05
Naja haje	0.57	0.30 – 1.08
Naja nivea	0.30	0.23 – 0.38

806

807

808

809

810

811

812

813

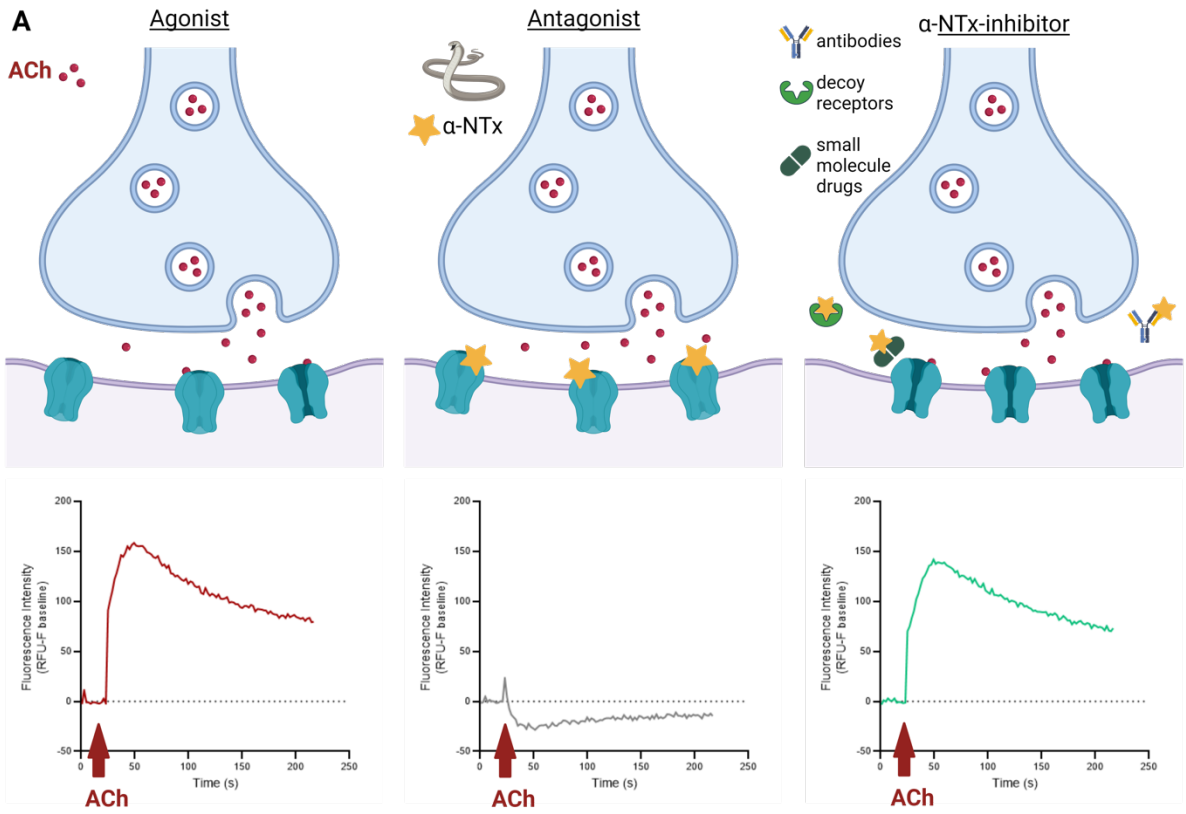

Fig. 1. Schematic of the neuromuscular junction and overview of corresponding readouts from the developed assay of nAChR activation. The schematics of the neuromuscular junction (top panels) demonstrate the release of ACh from the pre-synaptic neuron and binding of ACh to the post-synaptic membrane in the absence of α-NTxs (left, Agonist), in the presence of α-NTxs (middle, Antagonist), and in the presence of both α-NTxs and α-NTx-inhibitors (right, α-NTx-inhibitor). Underneath each illustration is the typical fluorescent response using the assay of a well in a 96-well plate containing TE671 cells when ACh alone (Agonist), ACh and α-NTx (Antagonist) and ACh, α-NTx and α-NTx-inhibitors (α-NTx-inhibitors: antibodies, decoy receptors, and small molecules) are added. All schematics were created with BioRender.

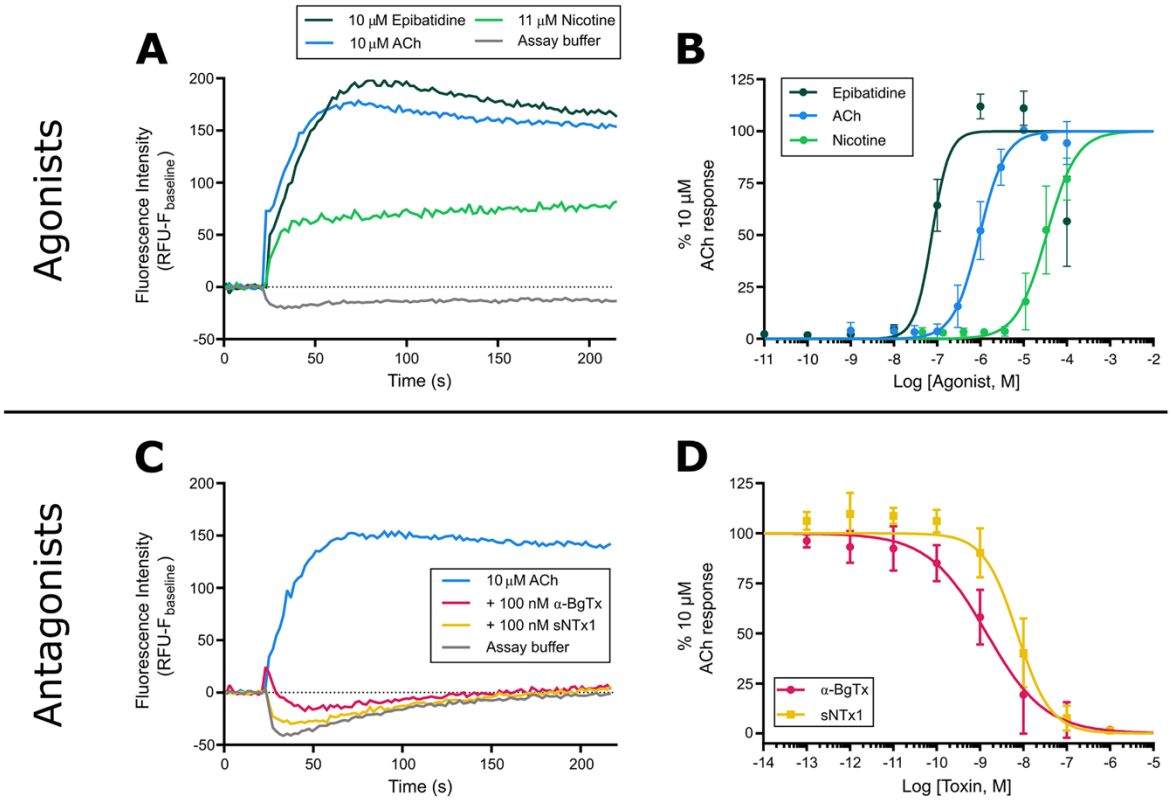

827

828 **Fig. 2. Known nAChR agonists and antagonists show expected action on TE671 nAChR**
829 **activation when using membrane potential dye.** (A) Representative traces showing changes
830 in fluorescence intensity of TE671 cells upon addition of nAChR agonists epibatidine (10 µM,
831 dark green), ACh (10 µM, blue), and nicotine (11 µM, light green), as well as assay buffer only
832 (grey), after 20 s baseline recording. (B) Concentration-response plots showing the changes in
833 the peak fluorescence intensity after addition of serial dilutions of epibatidine (dark green),
834 ACh (blue), and nicotine (light green). (C) Representative traces showing changes in
835 fluorescence intensity of TE671 cells after 15 min pre-incubation with 100 nM of the isolated
836 Lc-α-NTx α-BgTx (red) and the Sc-α-NTx sNTx1 (yellow), followed by addition of 10 µM
837 ACh after 20 s baseline recording. Representative traces of 10 µM ACh control (blue) and
838 assay buffer (grey) are also included. (D) Concentration-inhibition plots showing the inhibition
839 of peak fluorescence intensity of the 10 µM ACh response after the pre-incubation of serial
840 dilutions of α-BgTx (red) and sNTx1 (yellow). Each data point in (B) and (D) represents the
841 mean (±SD) of three independent experiments (n=3).

842

843

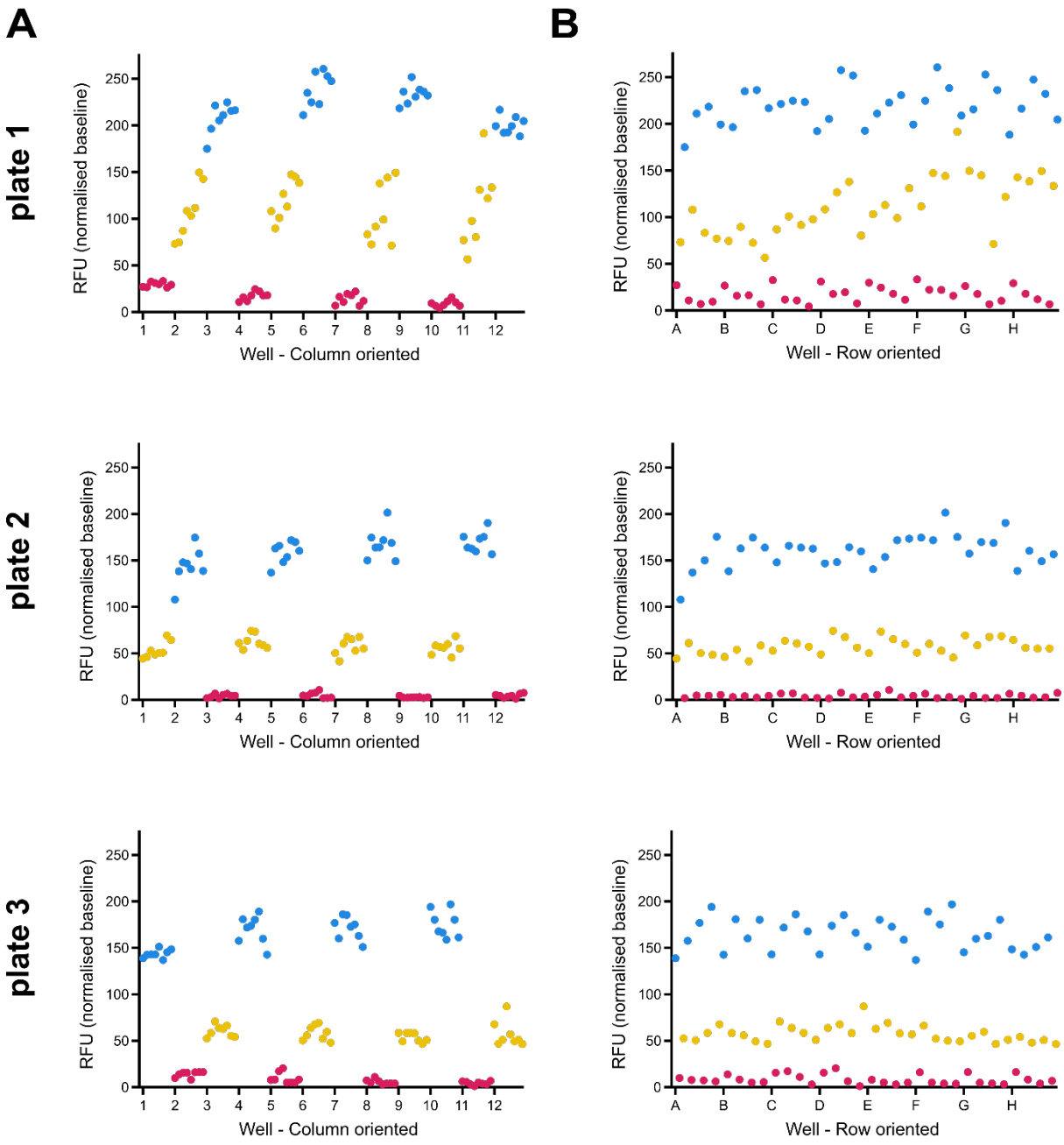

C

		Mean RFU			SD			CV			Mean RFU normalised to Max and Min controls		
		MIN	MID	MAX	MIN	MID	MAX	MIN	MID	MAX	MIN	MID	MAX
plate	1	17.5	111.2	220.1	8.7	31.2	21.3	8.8	5.0	1.7	0.0	46.2	100.0
	2	4.1	57.4	160.0	2.2	8.5	17.5	9.3	2.6	1.9	0.0	34.2	100.0
	3	8.5	57.4	165.0	5.2	8.9	17.3	10.9	2.7	1.9	0.0	31.2	100.0

Fig. 3. Responses of TE671 nAChRs with membrane potential dye are consistent across a 96-well plate. Scatter plots of the fluorescent response of TE671 cells from wells of a 96-well plate pre-incubated with concentrations of α-BgTx that either give maximal inhibition (30 nM, MIN, red), a middle level of inhibition (3 nM, MID, yellow), or no inhibition (none, MAX,

blue), followed by the addition of 10 µM ACh. Each condition was applied to alternating columns of three separate plates (n=3). Each row of plots contains data generated from one plate. Each plate was recorded on a different day with cells of a different passage number and the assigned MIN, MID, and MAX columns were changed on each plate. Each data point is the resulting RFU value after calculating F_{max}-$F_{baseline}$ and are plotted by column (A) or by row (B). (C) Summary table of the RFU mean, standard deviation (SD) and coefficient of variance (CV) for each control (MIN, MID, MAX) for each plate. The final column presents the RFU mean once normalised to the MIN and MAX controls.

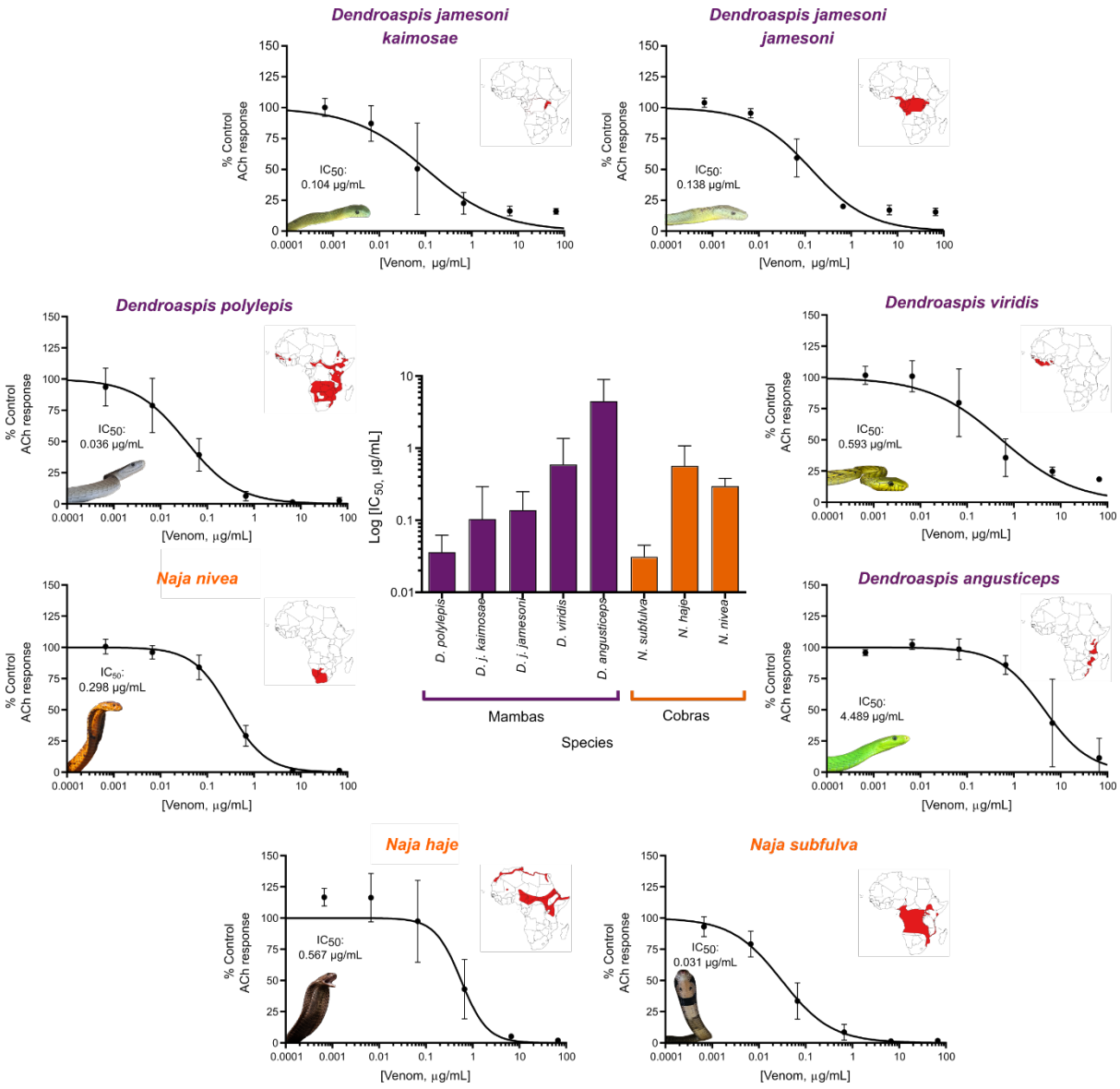

Fig. 4. Crude snake venoms show antagonism on nAChRs expressed in TE671 cells. Serial dilutions of crude venom (66.7 – 0.00067 µg/mL) extracted from neurotoxic elapid snake species with geographical distributions covering different regions of the African continent were pre-incubated with TE671 cells for 15 min followed by the addition of 10 µM ACh to create concentration-inhibition plots for each venom (outer ring). Each data point represents the mean (±SD) of three independent experiments (n=3). To the top right of each plot on the outer ring are maps of the African continent highlighting in red the geographical distribution of each species. Maps were generated using QGIS, based on the 2019 International Union for Conservation of Nature Red List of Threatened Species. The central plot compares the IC_{50} values (±95% CI) obtained from mamba (purple) and cobra (orange) venoms and IC_{50} values are displayed above images of snakes inset to the bottom left of each plot.

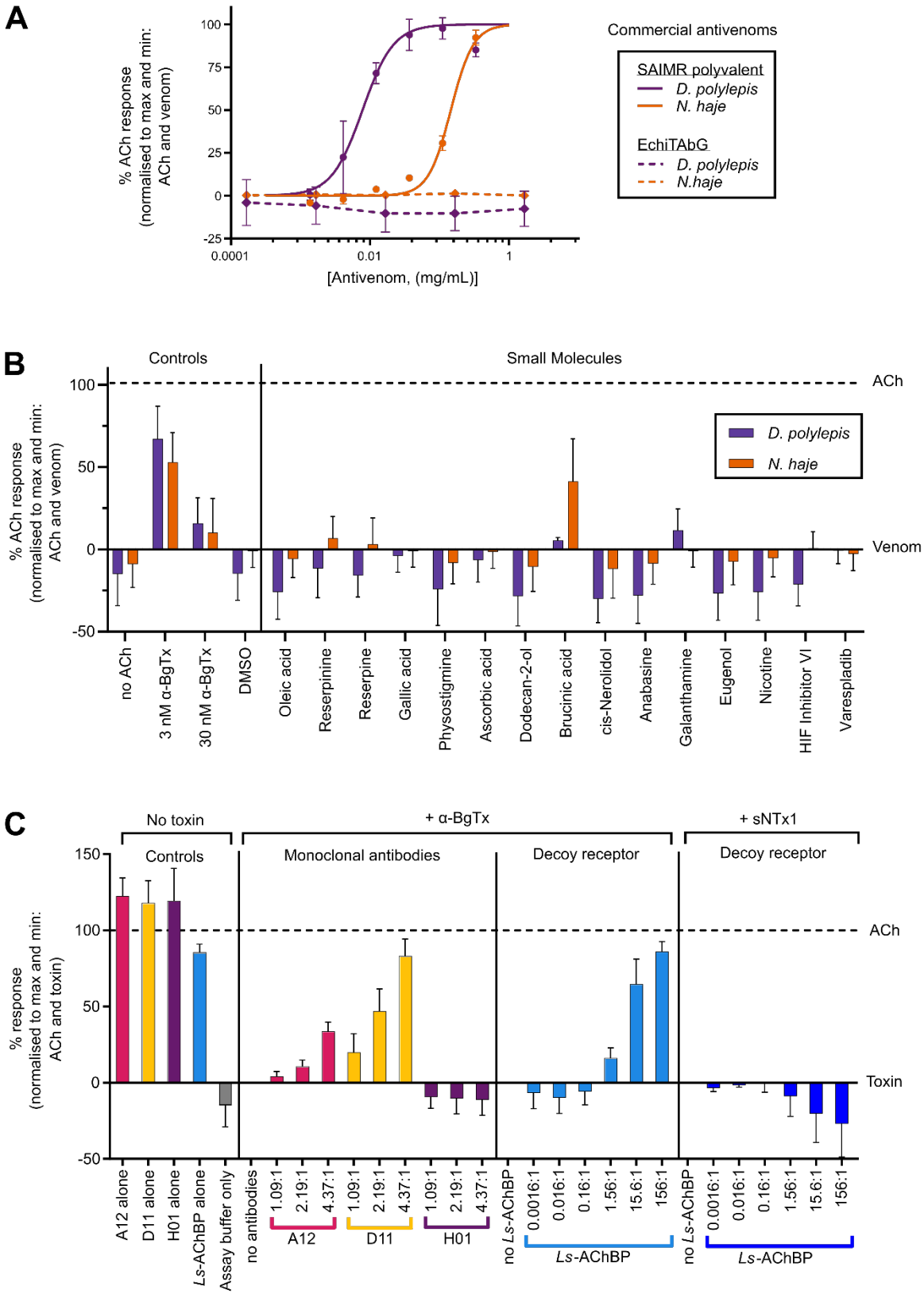

Fig. 5. Inhibition of venom or isolated α-NTxs by commercial antivenom, small molecules, monoclonal antibodies, and decoy receptors. α-NTx-inhibitors of various

formats were co-incubated with concentrations of crude venom (0.67 µg/mL for *D. polylepis* and 6.67 µg/mL for *N. haje*) or isolated α-NTx (30 nM) that gave approximate maximal inhibition prior to application to TE671 cells. All data points represent the mean (±SD) of three independent experiments (n=3) and are normalised to 10 µM ACh (100% signal) and ACh + venom/α-NTx (0% signal) controls with α-NTx-inhibitory activity represented by recovery towards the 100% ACh signal. Venom/α-NTx concentrations were constant at 6.67 and 0.67 µg/mL for *N. haje* and *D. polylepis* respectively. (A) Concentration-response curves showing TE671 ACh response after crude *D. polylepis* (purple) and *N. haje* (orange) venoms were co-incubated with serial dilutions of SAIMR polyvalent antivenom (solid lines, 333.3 – 1.4 µg/mL) and EchiTAbG (dotted lines, 1670.0 – 0.2 µg/mL). Only SAIMR polyvalent antivenom showed α-NTx-inhibiting activity with EC_{50}s of 7.8 µg/mL for *D. polylepis* and 146.1 µg/mL for *N. haje*. (B) Screening of a panel of rationally selected small molecules at 100 µM co-incubated with crude *D. polylepis* (purple) and *N. haje* (orange) venom. Each experiment included controls of assay buffer only (no ACh), 3 nM and 30 nM α-BgTx, and 1% DMSO as the drug vehicle control (DMSO). Only brucinic acid (NSC 121865) showed α-NTx-inhibiting activity after incubation with *N. haje* venom, but *D. polylepis* venom was not inhibited. (C) Serial dilutions of the 'decoy receptor' *Ls*-AChBP were pre-incubated with either 30 nM α-BgTx or 30 nM sNTx1 at molar ratios ranging from 156:1 – 0.0016:1 and dilutions of the mAbs 2551_01_A12 (A12) and 2554_01_D11 (D11) specific to Lc-α-NTXs, and 367_01_H01 (H01) specific to dendrotoxins were co-incubated with 30 nM α-BgTx at molar ratios of 4.37:1, 2.19:1 and 1.09:1. Inhibition of α-BgTx activity was observed after *Ls*-AChBP was co-incubated with α-BgTx at molar ratios of 156:1 – 1.56:1 but no inhibition of sNTx1 was observed after further dilution. Inhibition of α-BgTx activity was observed with only 2554_01_D11 (restoration to 83.1% of control ACh response with 4.37:1 ratio) and 2551_01_A12 mAbs, with 2554_01_D11 showing a greater level of α-NTx inhibition than 2551_01_A12 (restored to 83.1% of control response as opposed to 33.6% with 4.37:1 ratio). To ensure the α-NTx-inhibitors themselves had no effect on nAChR activation, controls of mAb only (2551_01_A12, 2554_01_D11, and 367_01_H01 alone) and *Ls*-AChBP only at the highest concentrations used for pre-incubation with α-NTxs were also included.